

Droplet-Microarray on Superhydrophobic-Superhydrophilic Patterns for High-Throughput Live Cell Screenings

Anna A. Popova¹, Konstantin Demir¹, Titus Genisius Hartanto¹, Eric Schmitt¹ and Pavel A. Levkin^{1}*

¹Karlsruhe Institute of Technology, Institute of Toxicology and Genetics, Hermann-von-Helmholtz-Platz 1, 76344 Eggenstein-Leopoldshafen, Germany

Correspondence should be addressed to P.A. Levkin: levkin@kit.edu

Keywords: Droplet-Microarray, superhydrophobic-superhydrophilic patterning, high throughput screenings of live cells

Abstract

Cell-based high content phenotypic screenings are widely used in fundamental research, pharmaceutical industry, and healthcare to simultaneously evaluate the effects of multiple compounds or gene over-expressions/knockdown on the phenotype of cells. Most screenings, especially in the industrial sector, are performed using microplate technology, which relies on high reagents and cell consumption as well as on expensive liquid handling robotics. Developing miniaturized screening platforms has been an important topic in the past decade. In this study we demonstrate the applicability of the Droplet-Microarray platform based on superhydrophobic-superhydrophilic patterning for cell-based high throughput screenings. We show the homogeneous seeding of cells and culturing of different adherent cell lines in individual droplets of different sizes. We demonstrate pipetting-free medium exchange enabling cell cultures in miniaturized droplet arrays for up to 5 days. We establish the method of reverse transfection and reverse drug screenings in individual nanoliter-size droplets by printing the transfection mixtures or drug molecules directly onto superhydrophilic spots prior to cell seeding.

Introduction

The high-throughput screening (HTS) of live cells is an immensely important method being increasingly applied in different scientific and industrial areas. It has raised the rate of scientific discoveries by enabling multiple parallel live cell experiments for the simultaneous evaluation of the effects of multiple factors on the phenotype of cells^{1,2}. Phenotypic cell-based screenings based on genetic perturbation of cells via RNA interference or gene over-expression are routine in fundamental science when investigating fundamental biological processes like cell signaling³, cell cycle control⁴, DNA repair machinery⁵, cell differentiation^{6,7}, apoptosis^{8,9} etc. HTS of live cells is widely employed in the pharmaceutical industry in fields such as drug discovery, antibody production and the toxicity testing of new drug candidates and bioactive compounds.

Most cell-based HTS are performed in 96- and 384-well microplates. Microplate technology has been and remains accepted as the most reliable platform for cell-based assays, however, it has several drawbacks. First, it offers low throughput and therefore requires high number of microplates. Plates with higher capacity (1536- and 3456-well plates) are also used, but due to problems associated with handling minute volumes, employing such plates can raise

the cost of screening¹⁰. Second, due to the relatively large sizes of individual wells, the plates are associated with high consumption of expensive reagents and valuable cells, making this valuable technology unaffordable for many research laboratories. In addition, requiring high quantities of cells makes it difficult or impossible to perform screenings on rare and hard-to-expand cells such as primary and stem cells. This is critical in the field of healthcare, where a minute amount of patient material is available. One of the main problems of microplate technology is that it requires multiple pipetting steps and, therefore, depends on expensive fluid handling robotic systems that are incompatible with miniaturization and personalized medicine.

In the past decade much has been done to miniaturize cell-based screenings by creating alternative platforms such as droplet microfluidic platforms¹¹⁻¹⁵, DropArray of Curiox, SlipChip¹⁶⁻²⁰, platforms based on hydrophobic-hydrophilic patterning²¹⁻²³ and miniaturized microplates²⁴⁻²⁷. Droplet microfluidics enables generation up to a billion homogeneous droplets encapsulating cells. This technology is widely used in applications such as the detection of cell metabolites²⁸, antibody screens²⁹, PCR³⁰ or sequencing^{14, 15}, and is compatible with high throughput compound screens using the “droplet library”³¹. However, droplet microfluidic technology might be inefficient for smaller assays³²; it does not have spatial indexing available as in two-dimensional arrays, thereby requiring the use of sophisticated bar coding to distinguish between droplets; it is incompatible with time lapse or end point microscopic analysis; and it makes it hard to study cells of adherent nature since they have no surface to interact with. SlipChip is an example of a microfluidic platform allowing the formation of two-dimensional arrays and microscopic analysis¹⁶. It permits the easy parallel and homogeneous spreading of cells, relying on the pipetting of multiple compounds into microfluidic paths³³. There are several groups utilizing hydrophobic-hydrophilic micropatterning to create arrays of cells encapsulated in droplets for screening applications²¹⁻²³. These are innovative and promising platforms for miniaturized cell-based screenings, however, they are still not compatible with high throughput format.

In 2001 Sabatini and colleagues developed cell microarrays and established a method of “reverse transfection”³⁴, a system based on preprinting an array of transfection mixtures containing nucleic acid onto a glass slide, followed by seeding a monolayer of adherent cells onto the glass surface. Cells growing on printed areas uptake the nucleic acid, creating a cluster of transfected cells. This methodology allows for parallel transfection of up to 10.000 cell clusters per standard microscope slide. Cell microarray technology thus permits high throughput parallel gene over-expression or knockout experiments, low reagent and cell consumption, and easy, pipetting-free handling. Many research groups adopted this method for their scientific discoveries^{2, 4, 8, 9}. Later applications of cell microarrays were extended to screenings of small drug like molecules. In this case drugs have to be embedded in polymer or lipids to prevent rapid diffusion of molecules into the media and ensure direct delivery of drugs into the cell cluster^{35, 36}. The main limitation of cell microarray technology is the absence of barriers between spots and the culturing of cells in one medium, which leads to risk of cross-contamination and paracrine interaction between cell clusters and restricts this technology to cells of adherent nature.

Recently we demonstrated that superhydrophobic-superhydrophilic patterning could be used to form high density arrays of microdroplets (Droplet-Microarray (DMA) platform)³⁷. We demonstrated the formation of droplet microarray using the effect of discontinuous dewetting³⁸,

the formation of arrays of hydrogel micropads³⁸ and DMA Sandwiching Chip for the parallel addition of chemical libraries to the individual droplets³⁷.

In this work we demonstrated how to solve the problems of the live cell microarrays developed by Sabatini using the inherent compartmentalization capability of the DMA platform. We showed the possibility of culturing HEK293, HeLa and A549 cell lines in arrays of droplets of 3 to 80 nL and demonstrated a single-step, pipetting-free medium exchange enabling cell culturing in droplet microcompartments up to 5 days. We established the method of reverse transfection and reverse small molecule drug screenings in individual droplets on the DMA. This combination of the parallelization, compartmentalization and miniaturization opens the way to extend the applications of live cell microarrays to small molecule screenings, drug screenings, reduce possible contamination problem and solve the problem of cell migration between the individual microwells.

Experimental

Fabrication of DMA slides

Preparation of superhydrophilic-superhydrophobic patterned surfaces was described elsewhere³⁸. Briefly, patterns were prepared as stated below.

Glass slide activation. Glass slides (Schott Nexterion, Jena, Germany) were activated by immersing in 1M NaOH (Carl Roth GmbH + Co. KG, Karlsruhe, Germany) for 1 hour followed by neutralization by immersing in 1M HCl (Merck KGaA, Darmstadt, Germany) for 30 minutes, followed by washing with DI water.

Glass slide modification. Activated glass slides were modified by spreading a small amount of 20% v/v ethanol solution of 3-(trimethoxysilyl)propyl methacrylate (Sigma-Aldrich, Munich, Germany) over activated glass slides and incubating them for 30 minutes, followed by washing with ethanol and drying under nitrogen stream.

Glass slide fluorination. Glass slides were fluorinated by storing them overnight under 50 mbar vacuum in a sealed desiccator containing an open 1,5 mL Eppendorf tube with 30 μ L of trichloro(1H, 1H, 2H, 2H-perfluorooctyl)silane (Sigma-Aldrich, Munich, Germany).

Polymer film preparation. To prepare a porous polymer layer, the following polymerization mixture was used: 24 wt.% 2-hydroxyethyl methacrylate (HEMA) (Sigma-Aldrich, Munich, Germany), 16 wt.% ethylene dimethacrylate (EDMA) (Sigma-Aldrich, Munich, Germany), 12 wt.% 1-decanol, 48 wt.% cyclohexanol (Sigma-Aldrich, Munich, Germany) and 0,4 wt.% 2,2-dimethoxy-2-phenylacetophenone (Sigma-Aldrich, Munich, Germany). To control the thickness of the polymer layer, 1,86 μ m monodispersed silica beads SiliaSphere 100Å (SiliCycle, Quebec, Canada) were applied on the corners of a fluorinated glass slide. Afterwards, the polymerization mixture was applied onto a fluorinated glass slide and covered with a modified slide. Polymerization occurred via UV irradiation of the glass mold with 260 nm UV light for 15 minutes at 7 mW/cm² intensity. Polymerization and surface patterning were carried out on an OAI Model 30 deep-UV collimated light source (Optical Associates Inc., San Jose, CA) fitted with an USHIO 500 W Hg-xenon lamp (Ushio, Tokyo, Japan). The fluorinated glass slide was then removed and the polymer surface washed with ethanol and dried with an air gun. To increase the polymer surface's roughness and therefore its hydrophobicity and hydrophilicity, the polymer's smooth superficial layer was removed by

applying an adhesive tape (EAN 4042448036223, Tesa, Offenburg, Germany) to its surface followed by rapid tape removal.

Surface patterning. Prior to patterning, the surface was modified by incubating the slides in solution containing 45 mL of dichloromethane (Merck KGaA, Darmstadt, Germany), 56 mg of 4-(dimethylamino)pyridine (Novabiochem, Merck KGaA, Darmstadt, Germany), 111,6 mg of 4-pentynoic acid (Sigma-Aldrich, Munich, Germany) and 180 μ L of *N,N'*-diisopropylcarbodiimine (Alfa Aesar, Karlsruhe, Germany) for 4 hours under stirring at room temperature. A superhydrophobic pattern was created by applying 5% v/v solution of 1H, 1H, 2H, 2H - Perfluorodecanethiol (Sigma-Aldrich, Munich, Germany) in acetone onto the polymer surface and irradiating the slide with 260 nm UV light at 7 mW/cm² for 1 min through a quartz photomask (Rose Fotomasken, Bergisch Gladbach, Germany). The polymer surface was extensively washed with acetone and dried with an air gun. Superhydrophilic spots were then created by applying 10% v/v β -mercaptoethanol (Alfa Aesar, Karlsruhe, Germany) solution in 1:1 v/v water:ethanol onto the patterned surface and irradiating the slide with 260 nm UV light at 7 mW/cm² for 1 min through a quartz slide.

Formation of droplet microarrays (“rolling droplet” method).

A large droplet of an aqueous solution was applied onto the patterned surface of a DMA slide (for 30 to 90 seconds in case of cell suspension) followed by slightly tilting of the slide, causing the droplet to roll off the surface spontaneously forming an array of separated droplets (Fig. 1b, Video S1). We refer to this method of forming a Droplet-Microarray as the “rolling droplet” method. SL spots on the DMA slide were divided into three fields surrounded by SH borders allowing for the application of a fixed volume of solution on one field, to ensure even droplets distribution across the slide and the experiment’s reproducibility.

Measuring droplet heights and calculating volumes of the droplets. To measure droplet height, water was spread onto a DMA slide and images of droplets were taken from the side using a camera with the telecentric measuring lens 62-932 (Edmund Optics GmbH, Karlsruhe, Germany). To minimize evaporation, imaging took place at 95% relative humidity in a sealed chamber equipped with a humidifier (Conrad Electronic, Hirschau, Germany) and humidity sensor (Galltec, Bondorf, Germany). The droplets’ height in the middle and width at the bottom were measured in pixels using ImageJ software. Knowing the width of the droplet’s footprint (equaling the size of the SL spot), the pixels were converted to μ m. The droplets’ approximate volume was calculated using the formula for volume of a spherical cap: $\left(\frac{\pi h}{6}\right)(3a^2 + h^2)$, where h is height of the droplet and a is size of superhydrophilic spot (droplet footprint) divided by two.

Alternatively, we estimated droplet volume by spreading the water on the slide and weighing it. Each droplet’s volume was calculated by dividing the total weight by the number of droplets.

Cell culture

Human embryonic kidney HEK293 cells, human cervical carcinoma HeLa cells and A549 cells were kindly provided by Dr. Olivier Kassel, Dr. Gary Davidson and Prof. Jonathan Sleeman (Institute of Toxicology and Genetics, KIT), respectively. HEK293, HeLa and A549 cells were cultured in complete Dulbecco’s Modified Eagle’s Medium DMEM (Gibco, Life

Technologies GmbH, Darmstadt, Germany) containing 10% of fetal bovine serum FBS (Sigma-Aldrich, Munich, Germany) and 1% of Penicillin/Streptomycin (Gibco, Life Technologies GmbH, Darmstadt, Germany). Cells were trypsinized using 0,25% trypsin/EDTA (Gibco, Life Technologies GmbH, Darmstadt, Germany) and split every 2-3 days at a ratio of 1/10 for HEK293 and A549 cells and 1/7 for HeLa cells, respectively.

Before seeding cells on DMA slides, the surfaces were prepared as follows. Patterns were sterilized in ethanol, dried and immersed in DMEM medium containing 1% FBS and 1% Penicillin/Streptomycin and incubated for 1 hour in a cell culture incubator at 37°C. Medium was aspirated and slides were dried for 1 hour under sterile hood. Afterwards, superhydrophilic spots were coated with 2,2% wt gelatin/water solution (Sigma-Aldrich, Munich, Germany). Patterns were incubated in cell culture incubator for 1 hour and dried under the sterile hood for 45 minutes. After preparation, slides could be used immediately or stored for up to three days in the fridge. To avoid droplet evaporation, the chamber for cell culturing was pre-humidified 30 minutes before starting an experiment according to the following procedure. For each DMA slide a sterile 100 mm Petri dish was placed inside another 150 mm Petri dish containing 10 mL of PBS and paper tissues placed along the circle of the dish. Such double Petri dishes were placed in cell culture incubator as a vertical stack and covered with sterile wetted paper tissues. Prior the cell seeding step, the double dish was taken out of an incubator and a preconditioned DMA slide was placed inside the sterile 100 mm Petri dish. Cells were seeded on the array field surrounded by the superhydrophobic border on a DMA slide by applying 1.7 mL of cell suspension containing the desired cell concentration (Table 1) (Fig. 1a). The Petri dish lid was closed to minimize evaporation and cells were allowed to settle for 30 seconds for HeLa and 90 seconds for HEK293 and A549 cells. Afterwards, the Petri dish with closed lid was slightly tilted to allow the cell-suspension droplet to roll off the surface of the DMA slide, leading to the spontaneous formation of droplets containing cells. The double Petri dish with DMA slide containing cells was immediately returned back to the stack in the cell culture incubator. The paper tissues covering the stack of double Petri dishes were wetted every day to keep local humid environment constant and prevent evaporation of the droplets.

Table 1. Seeding concentrations of cells used to achieve optimal initial cell density for cell proliferation and viability on DMA.

Cell type \ Spot size	1000 μm	500 μm	350 μm
HEK293	15x10 ⁴ cells/ mL	20x10 ⁴ cells/ mL	20x10 ⁴ cells/ mL
HeLa	25x10 ⁴ cells/ mL	50x10 ⁴ cells/ mL	100x10 ⁴ cells/ mL
A549	15x10 ⁴ cells/ mL	20x10 ⁴ cells/ mL	50x10 ⁴ cells/ mL

Studying the homogeneity of cell seeding

HeLa cells were seeded onto a DMA slide as described above and cultured in droplets for 5 hours to allow cells to attach to the surface. Afterwards, cells were fixed and stained by immersing the slide in a solution containing 3,7% formaldehyde, 0,1% triton, 0,5 $\mu\text{g}/\text{mL}$ DAPI in Dulbecco's phosphate buffered saline containing CaCl_2 and MgCl_2 (DPBS/ CaCl_2 / MgCl_2) (Gibco, Life Technologies GmbH, Darmstadt, Germany) for 15 minutes at room temperature. The slide was then mounted with Immu-Mount (Thermo Fisher Scientific Inc., Darmstadt,

Germany) and dried at +4°C. Images of each individual droplet were taken with an automated screening Olympus IX81 microscope (Olympus, Tokyo, Japan). DAPI stained nuclei were counted using CellProfiler (<http://www.cellprofiler.org/>).

Viability and cell growth study

All images for this study were taken using a Keyence BZ-9000 microscope (KEYENCE, Osaka, Japan). For proliferation and viability study, cells were seeded onto a DMA slide and ten spots were imaged immediately to estimate initial cell concentration. Afterwards, the same spots were imaged every 24 hours for up to 96 hours of culturing. Cells were counted manually using brightfield microscopy images. To distinguish between live and dead cells, HeLa cells were cultured in medium containing 100 nM Propidium Iodide (PI) (Invitrogene, Merelbeke, Belgium) to stain dead cells. In a separate experiment we confirmed that there was no difference in the growth and viability of HeLa cells with and without PI staining (data not shown). For HEK293 and A549 cell lines, cells showing well spread morphology were counted as live cells and those possessing round and shrunk morphology were considered as dead/apoptotic cells. The accuracy of such manual quantification was validated using double Calcein/PI staining. Each experiment was repeated at least three times.

Growth rates of HEK293, A549 and HeLa cells in 24 well plates were estimated as follows. Cells were plated in a 24-well plate with surface cell densities corresponding to those of a 1000 μm DMA slide, which were 90.500, 31.800 and 80.000 cells per well for HEK293, HeLa and A549, respectively. Every 24 hours, cells were detached from the surface with trypsin and counted using a hemocytometer (Assistant, Sondheim/Rhoen, Germany).

Reverse transfection

The following transfection mixture was prepared in a 384-well plate: 2.75 μL of ScreenFect Dilution Buffer (Incella GmbH, Eggenstein-Leopoldshafen, Germany) containing 0.4 M sucrose (Carl Roth GmbH, Karlsruhe, Germany), 6.25 μL 300 ng/ μL pCS2-H2B-GFP or pCS2-H2B-RFP in water (kindly provided by Dr. Gary Davidson, Institute of Toxicology and Genetics, KIT), 5 μL ScreenFect[®]A (Incella GmbH, Eggenstein-Leopoldshafen, Germany) and 4.65 μL ScreenFect Dilution Buffer. The mixture was incubated for 20 minutes at room temperature to allow formation of lipoplexes. Afterwards, 3.75 μL of 0.1% solution of fibronectin in water (VWR International GmbH, Germany) and 7.5 μL of 0.2% solution of gelatin in water (Sigma-Aldrich, Munich, Germany) were added to the mixture. Then the transfection mixture was printed onto the DMA slide's SL spots using a sciFLEXARRAYER S11 liquid dispenser (Scienion, Berlin, Germany) in amounts of 20 nl, 40 nl and 150 nl for DMA slides with spots measuring 350 μm , 500 μm , and 1000 μm , respectively. Slides were dried in a closed desiccator containing silica gel (Sigma-Aldrich, Munich, Germany) for 2 days in case of 350 and 500 μm spot sizes, and for 5 days in case of the 1000 μm spot size. Cells were seeded onto the DMA slide with preprinted transfection mixtures as described above. Transfection efficiency was estimated 24 and 48 hours after seeding by live imaging.

“Reverse” drug treatment

Water solution of doxorubicin (European Pharmacopolia Reference Standard, EDQM, Strasbourg, France) was printed onto the SL spots on DMA slides using a sciFLEXARRAYER S11 liquid dispenser (Scienion, Berlin, Germany) in amounts 25, 7, 5, 3, 2 ng per spot. DMA

slides with preprinted drug were dried in a sealed desiccator containing silica gel (Sigma-Aldrich, Munich, Germany) for 24 hours. Cells were seeded onto DMA slides containing doxorubicin as described above. The effect of doxorubicin was evaluated 24 hours after seeding via live staining with Calcein AM (Life Technologies GmbH, Darmstadt, Germany). Staining was done by “sandwiching” a DMA slide containing cells with an identical pattern, where 50 μ M solution of Calcein AM in Dulbecco’s Phosphate Buffered Saline containing CaCl_2 and MgCl_2 (DPBS/ CaCl_2 / MgCl_2) (Gibco, Life Technologies GmbH, Darmstadt, Germany) was spread, for 10 minutes. Slides were then separated, and the DMA slide placed in a cell culture incubator for 15 minutes. Images of treated spots were taken using the Keyence BZ-9000 microscope (KEYENCE, Osaka, Japan). The number of live cells stained green was counted using CellProfiler (<http://www.cellprofiler.org/>).

Results

Droplet-Microarray Reverse Screening Platform

The design of a Droplet-Microarray (DMA) slide is shown in Fig. 1a. A standard microscope glass slide was covered with a nanoporous poly(2-hydroxyethyl methacrylate-*co*-ethylene dimethacrylate) (HEMA-EDMA) film and esterified using 4-propynoic acid. The porous DMA surface was then functionalized via thiol-yne reaction with 2-mercaptoethanol to make differently-sized superhydrophilic (SL) square spots and with perfluorodecanthiol to make superhydrophobic (SH) borders of corresponding sizes (Fig. 1a).³⁹ The DMA slides contained 588, 2187 or 4563 SL spots per slide in case of spots measuring 1000 μ m, 500 μ m and 350 μ m, respectively. Because of the extreme difference in wettability between SL (static water contact angle 4.4°) and SH (static water contact angle 170°), SL spots can be filled with water-based solution in a single step via the effect of discontinuous dewetting (Fig. 1 b-c)³⁷⁻⁴⁰. Here the ability to create thousands of separated aqueous micro-compartments in a single step was used to establish and evaluate the DMA for *reverse cell screening* applications (Fig. 1c).

The screening pipeline using DMA is depicted in Fig. 1c. First, substances of interest such as drugs or transfection mixtures are printed onto SL spots using a conventional non-contact liquid dispenser and dried. To start a cell screen, a pre-printed SH-SL slide is used to form an array of separated microdroplets in one step *via* the “rolling droplet” method (Fig. 1c, Video S1, experimental part). Once droplets have formed, the preprinted chemicals dissolve in the individual microdroplets containing live cells, leading to changes in their phenotype that can be analyzed using conventional techniques such as fluorescence microscopy or array scanners. As shown in Fig. 1c, in case of adherent cells, DMA slides can be fully immersed into a solution for washing, staining or fixation procedures. On the other hand, each droplet can be also treated individually by applying the sandwich method when staining, washing, or fixation solution is spread onto identical DMA slide and then added to droplets containing cells by sandwiching³⁷ (Fig. 1c). This is important, for example, when using non-adherent cells where each droplet’s content must be preserved. As a final step, phenotype changes in cells are analyzed using fluorescence microscopy (Fig. 1c).

Homogeneous droplet formation and cell seeding on DMA

The pipetting-free homogeneous formation of thousands of droplets in array format is indispensable for various screening applications whereby substances, particles, or cells must be

evenly distributed between compartments. To monitor the distribution of droplet volumes, we imaged water droplets formed on a DMA slide from the side to measure their heights (Figs. 2a, b). As Fig. 2a illustrates, the droplets' heights measured 195 ± 25 , 90 ± 23 and 64 ± 10 μm for patterns with 1000 μm , 500 μm and 350 μm spots, respectively. Using the equation of the volume of spherical cap, volumes of droplets formed in 1000, 500 and 350 μm SL spots were estimated to number 81 ± 18 , 9.3 ± 2 and 3.25 ± 0.5 nL, respectively. This estimation was confirmed by measuring the droplets' average volume by weighing water spread on a DMA slide containing a certain number of formed droplets. This method yielded very similar droplet-volume values (84.5 ± 14 , 9 ± 1 and 3.4 ± 0.2 nL for 1000, 500 and 350 μm SL spots, respectively).

In the next step we investigated the possibility of creating an array of homogeneously distributed cells in droplets. Human cervical carcinoma cells (HeLa) were seeded onto a DMA slide using the "rolling droplet" method (experimental part) and incubated for several hours to allow cells to attach to the surface. To calculate the number of cells in each droplet, cells were fixed, stained with DAPI, and subjected to automated microscope imaging and analysis (Fig. 2c-e). Droplets contained 163 ± 33 , 57 ± 17 and 26 ± 16 cells for DMAs with spot sizes of 1000, 500 and 350 μm , respectively (Figs. 2c-e). Color-coded maps of distribution of cell numbers reveal that cells were spread randomly across the slide (except the corner spots), that the number of cells per droplet did not depend on the position on the field, and was unaffected by the cell-spreading technique (Figs. 2c-e). We observed spots containing less than 10 cells on DMA with 350 μm spot size, which can be explained by inhomogeneity of the initial cell suspension and small volume of the droplets.

Cell culturing on Droplet-Microarray

To evaluate the DMA platform for cell-based screening we optimized culturing conditions in individual droplets using three common cell lines: a human cervical cancer cell line (HeLa), human embryonic kidney cell line (HEK293), and human lung adenocarcinoma epithelial cell line (A549). To prepare the DMA slide to culture cells, we first immersed it in DMEM medium containing 1% FBS, followed by coating SL spots with 2.2% wt. gelatin. Droplet microarray was formed and the array was placed in a cell culture incubator in a humidified double Petri dish to prevent evaporation. All three cell lines cultured in individual droplets of different sizes for 24 hours revealed spread morphology similar to that of cells cultured in microplates (Fig. 3) and viability of cells in droplets was 97-100% as proven by live/dead staining (Fig. S1e).

For screening applications where the effect of chemicals on cell phenotype might develop in hours or days, it is important to be able to culture cells for several days. To observe how long cells can be cultured on DMAs without medium exchange, we monitored cell viability and the growth rates of HEK293, A549 and HeLa cells cultured in individual droplets of different sizes for five days (Fig. 4, Fig. S2). We noted that the rate of cell growth depended strongly on the initial cell concentration (Fig. S1a). We therefore experimentally defined the initial cell concentration for optimal cell growth for each cell line (Table 1). As demonstrated in Fig. 4b-d, cells proliferated for up to 48 hours on 1000 μm pattern and up to 24 hours on 500 μm and 350 μm patterns. All three cell lines grew slower in individual droplets compared to a 24-well microplate (Fig. S1d). This can be explained by the fact that the volume of medium per cell is approximately 30 times lower in droplets than in a well in a 96-well plate with the same density of cells per area. Nevertheless, the viability of cells in droplets after 24 hours of

culturing ranged from 95 to 100% depending on the cell line and spot size, similar to the viability of cells in microplates (Fig. S1e). Depending on cell line, viability of cells after 48 hours of culturing was 86-100%, 69-97% and 63 to 100% on DMA with spot sizes 1000 μm , 500 μm and 350 μm spot sizes, respectively (Fig. S1e).

As a next step we explored the potential of medium exchange on the DMA platform. Medium exchange is usually difficult in miniaturized cell screening systems, such as droplet microfluidics. The DMA platform is an open system, contrary to most of the microfluidic systems and, therefore, medium can be easily exchanged using the “rolling droplet” method (Fig. 4a, Video S1). Briefly, 1,7 mL of fresh medium was applied onto one of three fields on a DMA slide, followed by tilting the slide slightly to allow the medium to roll off the surface, thereby forming individual droplets with fresh medium. As depicted in Fig. 4 b-d, medium exchange prolonged cell proliferation inside the droplets for up to 96 hours (Fig. 4b-d). Although the growth rate of HeLa cells in droplets was still lower than in microplates, cells remained high viability comparable with that of cells cultured in microplates (Fig. 4b-d). Considering these factors together, we can conclude that it is possible to perform screening of live cells using the DMA platform with 1000 μm , 500 μm and 350 μm spot sizes for up to 48 hours without medium exchange and for up to 96 hours in case of daily medium exchange.

Reverse Cell Transfection and Drug Screening

High-throughput gain- or loss-of-function cell experiments are key to understanding gene and protein functions^{2, 4, 8, 9}. Most of such HTS experiments are performed either using standard microplates or using Sabatini’s reverse cell transfection arrays. Combining the compartmentalization advantage of the DMA with the high throughput and the pipetting-free nature of the reverse cell transfection method would be beneficial to extend the scope of the reverse transfection to other cell screen types. Here, we optimized the method of reverse transfection using the DMA platform. Transfection mixtures containing transfection reagent, plasmid DNA expressing H2B-YFP or H2B-RFP, buffer and gelatin were printed onto SL spots using a non-contact liquid dispenser (Fig. 5a). Slides were dried in a desiccator for 3 days and 5 days in case of 1000 μm and 500/350 μm spots, respectively. HEK293 cells were seeded on the DMA slide to create an array of droplets, and transfection efficiency was assessed 24 hours after seeding using fluorescence microscopy (Fig. 5). HEK293 cells were successfully transfected with plasmids expressing H2B-YFP and H2B-RFP with transfection efficiency from 50 to 80% (Fig. 5). For comparison the transfection efficiency of ScreenFect transfection reagent in 96 well plate using conventional transfection protocol is from 60 to 90%. As shown on Fig. 5b, there was no cross-contamination between the spots during the seeding procedure, although the superhydrophobic gap between the SL spots measured only 175 μm for the 350 μm array.

Previously we demonstrated the parallel simultaneous addition of drugs into individual droplets on a DMA slide using the “sandwiching method”³⁷. In this study we introduced small-molecule drugs to individual droplets using a “reverse” approach by pre-printing chemicals onto SL spots before an experiment. To prove the absence of cross-contamination between spots during the seeding procedure, a water solution of the antineoplastic drug doxorubicin was printed onto SL spots on DMA slides with three different spot sizes in a checkerboard pattern amounting to 25 ng per spot. Slides were dried in a desiccator overnight, and an array of droplets was formed using the “rolling droplet” method by applying 1.7 mL of water for 30 seconds,

then slightly tilting the slide to make the big droplet roll off the surface, thus forming the droplet array (Fig. 6a, Video S1). Fluorescence images of the slide before and after droplet array formation (Fig. 6b-c, Fig. S3) confirmed that there was no cross-contamination between the spots in conjunction with water solution of doxorubicin, even for 350 μm spots with only 175 μm SH barriers.

In the next step, we introduced HeLa cells to doxorubicin using the “reverse approach”. Doxorubicin was pre-printed onto the DMA slide with 1000 μm hydrophilic spots in a checkerboard pattern (25 ng per spot). HeLa cells were seeded onto this slide using the “rolling droplet” method. The drug’s effect was quantified 24 hours after treatment by Calcein staining. As shown in Figs. 7a and b, spots with printed doxorubicin contained few or no live cells. In contrast, spots without doxorubicin were full of live cells (Figs. 7b and c). Cell viability is quantified in Fig. 7d. To exclude the influence of doxorubicin on cells cultured in neighboring spots not containing the drug, we compared the viability of cells in those droplets with that of cells on a slide not containing the drug. Figure 7d reveals that there was no difference in the number of live cells on these two DMAs, confirming that cross-contamination between droplets during the seeding procedure or culturing period does not occur (Fig. 7d). To prove that we can control concentration of doxorubicin in droplets, HeLa cells were introduced to doxorubicin preprinted in amounts ranging from 2 to 7 ng per spot, resulting in the final concentration of doxorubicin in droplets ranging from 46 to 161 μM . Figure 7e demonstrates the concentration-dependent effect of doxorubicin on the viability of HeLa cells. IC₅₀ of doxorubicin calculated based on these results equals 63.9 μM . We previously showed that the IC₅₀ value of doxorubicin on HeLa cells determined using the same experimental setup (cell density per area and incubation time with the drug) in 96 well plates was 3 μM ³⁷. The increase of IC₅₀ in the droplet microarray system can be explained by higher “culture medium volume” to “cell number” ratio in microplates compared to the droplet microarray system. In other words, although the concentration of doxorubicin was the same in the droplets and in the microwells, the total amount of the drug per single cell was significantly lower in the case of the droplet microarray platform. In general IC₅₀ value of a drug can vary significantly depending on experimental setup: according to the literature IC₅₀ value of doxorubicin in HeLa cells was found to be 0.2 μM ⁴¹, 3.7 μM ⁴² and 16.7 μM ⁴³.

Discussion and conclusion

In current study we explored the potential of Droplet-Microarray as a miniaturized technology for high content cell-based screens and demonstrated the suitability of the platform for cell-based screening applications.

We fabricated arrays containing square superhydrophilic spots with side lengths of 1000 μm , 500 μm and 350 μm , which could trap droplets of 80, 9 and 3 nL, respectively, which require 1000, 10.000 and 30.000 times less medium and reagents comparing to 96-well microplates and about 600, 5.000 and 15.000 times less medium and reagents comparing to 384-well microplates. Each spot has a 30- (1000 μm), 130- (500 μm) and 260- (350 μm) times smaller surface area compared to wells in a 96-well microplate, which is reflected in lower cell consumption for a single experiment. In addition to minute reagent and cell consumption DMA offers higher throughput. For comparison one DMA with the same area as microtiter plate can contain from 3.500 to 29.000 spots depending on spot size, which means that one DMA can potentially substitute up to 75 384-well plates. Thus, due to minute reagent consumption and

higher throughput, DMA allows for dramatic decrease in the total cost of cell screening experiments.

The minimal variation in initial condition is important for achieving reliable screening data and we were able to demonstrate that Droplet-Microarray created by spontaneous droplet formation has homogeneous distribution of droplet volumes and cell numbers between droplets. It should be noted that variation in initial cell densities per droplet was higher in smaller droplets (350 μm) if compared to bigger droplets (1000 μm). Initial cell number can be a critical parameter and therefore the spot size should be carefully validated for particular screening and read-out protocols.

We demonstrated the culturing of different adherent cell lines in individual droplets of different sizes. Pipetting-free medium exchange enabling cell cultures in miniaturized droplet arrays for up to 5 days was introduced. We demonstrated that cells proliferated on a DMA for up to 48 hours without medium exchange and up to 96 hours in case of medium exchange. Medium exchange is a challenge for most of the miniaturized cell compartmentalization technologies. The advantage of the DMA platform is that the system is open and, thus, facile medium exchange is possible by the rolling droplet method (Fig. 4a). It should be noted though that exchange of the medium requires coverage of the whole slide with medium for a few seconds, which can potentially lead to washing off dead or semi-adherent cells and might lead to cross-contamination. Therefore medium exchange would not be compatible with some protocols. In this case DMA can be used for protocols requiring up to 48 hours. Considering that many screening protocols (including drug screenings, gene-overexpression and gene silencing) are carried out within 24 to 48 hours^{2, 4, 8, 9}, DMA can be a suitable platform for various screening applications.

We demonstrated the applicability of the DMA platform for reverse cell transfection and reverse drug screenings in individual droplet microcompartments formed by discontinuous dewetting. The main advantage of the DMA platform compared to cell microarrays is screening of cells in completely separated micro compartments, which eliminates the problem of cross-contamination and paracrine interaction between spots during the culturing period; and enables the screening of cells of non-adherent nature. Thereby, we combined the compartmentalization advantage of the DMA with the high throughput and the pipetting-free nature of the method of reverse cell transfection. Such unique combination enables us to extend the scope of the reverse transfection to broader cell screening applications.

Routine low- to medium-throughput screenings are often performed manually using microplates and without the help of pipetting robots. The use of the DMA platform in such cases can make these experiments much faster and significantly cheaper. The initiation of a screening is performed simultaneously with the cell seeding step on a DMA slide and takes only several seconds. In case of using microtiter plate every well has to be pipetted individually first to seed cells and then to add chemical compounds. Using 384-well plate it might take several minutes to seed cells using a 16-channel pipette and about an hour to initiate the screening. In addition, manual pipetting is associated with higher well-to-well variations. Finally, there is a time gap between seeding cells and initiation of a screen in the first well of the first plate and the last well of the last plate, which can affect the outcome of the screening especially in case of short incubation times. In pharmaceutical companies screenings are performed with the help of robotics, where the well-to-well variations are minimized and the protocols are well established. The costs of establishing a new screening system must be taken into account when

considering switching to a miniaturized technology. However, considering that big companies screen about 100.000 compounds a day¹⁰, the dramatic reduction of the total cost of experiments can be still beneficial when switching to a new system.

Due to low cell consumption Droplet-Microarray can be used for performing screenings of rare and difficult to expand cells, such as primary or stem cells. Such screens can be useful for research purposes as well as in healthcare and can be difficult or impossible to perform using standard microplates. One example of such a screen is the drug sensitivity and resistance assay based on testing patient's tumor cells against a library of anti-cancer compounds to predict optimal therapy for this particular patient⁴⁴⁻⁴⁶. Such assays performed in 96- or 384-well plates are restricted because of the limited patient's tumor cell material available. The DMA platform carries a potential to be applied in such tests since it enables screenings of minute amounts of tumor cells and at the same time it is compatible with screening of larger chemical libraries.

In summary, DMA screening platform enables (1) miniaturization (1000 times less reagent consumption than a regular 96-well plate); (2) high-throughput (up to 4.500 spots per microscope slide); (3) compartmentalization (no cross-contamination or paracrine interaction between spots; compatibility with both adherent and non-adherent cells) and (4) simultaneous pipetting-free cell seeding and initiation of screening. As any new technology Droplet-Microarray needs to go through proof-of-concept initial phase to evaluate, validate and improve a technology as well as demonstrate its potential applications. We believe that Droplet-Microarray platform has a great potential to be commercialized and become available to any biological lab. In this case the ready-to-use DMA slides with custom preprinted chemical libraries would be purchased and screening would be affordable and easy to perform. We believe that for certain applications it will become easier and cheaper to perform cell-based high-throughput screenings using DMA technology than it is now using microtiter plates.

Acknowledgements

The research was supported by the ERC Starting Grant (ID: 337077-DropCellArray) and the Helmholtz Association's Initiative and Networking Fund (Grant No. VH-NG-621). The authors are grateful to Dr. Gary Davidson, Dr. Olivier Kassel and Prof. Jonathan Sleeman (Institute of Toxicology and Genetics, KIT) for providing the cell lines.

References

1. R. P. Hertzberg and A. J. Pope, *Current Opinion in Chemical Biology*, 2000, **4**, 445-451.
2. K. Papp, Z. Szittner and J. Prechl, *Cellular and Molecular Life Sciences*, 2012, **69**, 2717-2725.
3. J. Downward, *Oncogene*, 2004, **23**, 8376-8383.
4. B. Neumann, T. Walter, J. K. Hérliche, J. Bulkescher, H. Erfle, C. Conrad, P. Rogers, I. Poser, M. Held, U. Liebel, C. Cetin, F. Sieckmann, G. Pau, R. Kabbe, A. Wunsche, V. Satagopam, M. H. Schmitz, C. Chapuis, D. W. Gerlich, R. Schneider, R. Eils, W. Huber, J. M. Peters, A. A. Hyman, R. Durbin, R. Pepperkok and J. Ellenberg, *Nature*, 2010, **464**, 721-727.
5. D. M. Weingeist, J. Ge, D. K. Wood, J. T. Mutamba, Q. Huang, E. A. Rowland, M. B. Yaffe, S. Floyd and B. P. Engelward, *Cell Cycle*, 2013, **12**, 907-915.
6. S. C. Desbordes, D. G. Placantonakis, A. Ciro, N. D. Socci, G. Lee, H. Djaballah and L. Studer, *Cell stem cell*, 2008, **2**, 602-612.
7. F. Yamauchi, M. Okada, K. Kato, L. M. Jakt and H. Iwata, *Biochimica et Biophysica Acta (BBA) - General Subjects*, 2007, **1770**, 1085-1097.
8. O. Mannherz, D. Mertens, M. Hahn and P. Lichter, *Genomics*, 2006, **87**, 665-672.

9. E. L. Palmer, A. D. Miller and T. C. Freeman, *BMC Genomics*, 2006, **7**, 145-145.
10. A. Smith, *Nature*, 2002, **418**, 453-459.
11. Z. Wang, M.-C. Kim, M. Marquez and T. Thorsen, *Lab on a Chip*, 2007, **7**, 740-745.
12. J. Clause-Tormos, D. Lieber, J. C. Baret, A. El-Harrak, O. J. Miller, L. Frenz, J. Blouwolff, K. J. Humphry, S. Koster, H. Duan, C. Holtze, D. A. Weitz, A. D. Griffiths and C. A. Merten, *Chem Biol*, 2008, **15**, 427-437.
13. V. Lecault, M. VanInsberghe, S. Sekulovic, D. J. H. F. Knapp, S. Wohrer, W. Bowden, F. Viel, T. McLaughlin, A. Jarandehi, M. Miller, D. Falconnet, A. K. White, D. G. Kent, M. R. Copley, F. Taghipour, C. J. Eaves, R. K. Humphries, J. M. Piret and C. L. Hansen, *Nat Meth*, 2011, **8**, 581-586.
14. Evan Z. Macosko, A. Basu, R. Satija, J. Nemes, K. Shekhar, M. Goldman, I. Tirosh, Allison R. Bialas, N. Kamitaki, Emily M. Martersteck, John J. Trombetta, David A. Weitz, Joshua R. Sanes, Alex K. Shalek, A. Regev and Steven A. McCarroll, *Cell*, 2015, **161**, 1202-1214.
15. Allon M. Klein, L. Mazutis, I. Akartuna, N. Tallapragada, A. Veres, V. Li, L. Peshkin, David A. Weitz and Marc W. Kirschner, *Cell*, **161**, 1187-1201.
16. W. Du, L. Li, K. P. Nichols and R. F. Ismagilov, *Lab on a chip*, 2009, **9**, 2286-2292.
17. F. Shen, W. Du, E. K. Davydova, M. A. Karymov, J. Pandey and R. F. Ismagilov, *Analytical chemistry*, 2010, **82**, 4606-4612.
18. W. Liu, D. Chen, W. Du, K. P. Nichols and R. F. Ismagilov, *Analytical chemistry*, 2010, **82**, 3276-3282.
19. L. Ma, S. S. Datta, M. A. Karymov, Q. Pan, S. Begolo and R. F. Ismagilov, *Integrative biology : quantitative biosciences from nano to macro*, 2014, **6**, 796-805.
20. C.-W. Chang, C.-C. Peng, W.-H. Liao and Y.-C. Tung, *Analyst*, 2015, DOI: 10.1039/C5AN00547G.
21. M. B. Oliveira, A. I. Neto, C. R. Correia, M. I. Rial-Hermida, C. Alvarez-Lorenzo and J. F. Mano, *ACS Applied Materials & Interfaces*, 2014, **6**, 9488-9495.
22. A. I. Neto, C. A. Custodio, W. Song and J. F. Mano, *Soft Matter*, 2011, **7**, 4147-4151.
23. H. Li, Q. Yang, G. Li, M. Li, S. Wang and Y. Song, *ACS Applied Materials & Interfaces*, 2015, **7**, 9060-9065.
24. S. Lindström, R. Larsson and H. Andersson Svahn, *ELECTROPHORESIS*, 2008, **29**, 1219-1227.
25. S. Lindström, M. Eriksson, T. Vazin, J. Sandberg, J. Lundeberg, J. Frisé and H. Andersson-Svahn, *PLoS ONE*, 2009, **4**, e6997.
26. S. Yamamura, H. Kishi, Y. Tokimitsu, S. Kondo, R. Honda, S. R. Rao, M. Omori, E. Tamiya and A. Muraguchi, *Analytical Chemistry*, 2005, **77**, 8050-8056.
27. J. Wu, I. Wheeldon, Y. Guo, T. Lu, Y. Du, B. Wang, J. He, Y. Hu and A. Khademhosseini, *Biomaterials*, 2011, **32**, 841-848.
28. B. L. Wang, A. Ghaderi, H. Zhou, J. Agresti, D. A. Weitz, G. R. Fink and G. Stephanopoulos, *Nat Biotech*, 2014, **32**, 473-478.
29. S. Koster, F. E. Angile, H. Duan, J. J. Agresti, A. Wintner, C. Schmitz, A. C. Rowat, C. A. Merten, D. Pisignano, A. D. Griffiths and D. A. Weitz, *Lab on a Chip*, 2008, **8**, 1110-1115.
30. Y. Zeng, R. Novak, J. Shuga, M. T. Smith and R. A. Mathies, *Analytical Chemistry*, 2010, **82**, 3183-3190.
31. E. Brouzes, M. Medkova, N. Savenelli, D. Marran, M. Twardowski, J. B. Hutchison, J. M. Rothberg, D. R. Link, N. Perrimon and M. L. Samuels, *Proceedings of the National Academy of Sciences of the United States of America*, 2009, **106**, 14195-14200.
32. M. T. Guo, A. Rotem, J. A. Heyman and D. A. Weitz, *Lab on a Chip*, 2012, **12**, 2146-2155.
33. C. Shen, P. Xu, Z. Huang, D. Cai, S.-J. Liu and W. Du, *Lab on a Chip*, 2014, **14**, 3074-3080.
34. J. Ziauddin and D. M. Sabatini, *Nature*, 2001, **411**, 107-110.
35. S. N. Bailey, D. M. Sabatini and B. R. Stockwell, *Proceedings of the National Academy of Sciences of the United States of America*, 2004, **101**, 16144-16149.
36. A. E. Kusi-Appiah, N. Vafai, P. J. Cranfill, M. W. Davidson and S. Lenhart, *Biomaterials*, 2012, **33**, 4187-4194.
37. A. A. Popova, S. M. Schillo, K. Demir, E. Ueda, A. Nesterov-Mueller and P. A. Levkin, *Advanced Materials*, 2015, **27**, 5217-5222.

38. E. Ueda, F. L. Geyer, V. Nedashkivska and P. A. Levkin, *Lab on a Chip*, 2012, **12**, 5218-5224.
39. W. Feng, L. Li, E. Ueda, J. Li, S. Heißler, A. Welle, O. Trapp and P. A. Levkin, *Advanced Materials Interfaces*, 2014, **1**, n/a-n/a.
40. R. J. Jackman, D. C. Duffy, E. Ostuni, N. D. Willmore and G. M. Whitesides, *Analytical Chemistry*, 1998, **70**, 2280-2287.
41. S. K. Wattanapitayakul, L. Chularojmontri, A. Herunsalee, S. Charuchongkolwongse, S. Niumsakul and J. A. Bauer, *Basic & Clinical Pharmacology & Toxicology*, 2005, **96**, 80-87.
42. H. Sadeghi-Aliabadi, M. Minaiyan and A. Dabestan, *Research in Pharmaceutical Sciences*, 2010, **5**, 127-133.
43. N. Tong, J. I. E. Zhang, Y. Chen, Z. Li, Y. Luo, H. U. A. Zuo and X. Zhao, *Oncology Letters*, 2012, **3**, 1263-1267.
44. K. Brigulová, M. Červinka, J. Tošner and I. Sedláková, *Toxicology in Vitro*, 2010, **24**, 2108-2115.
45. Y. Iwadate, S. Fujimoto, H. Namba and A. Yamaura, *Br J Cancer*, 0000, **89**, 1896-1900.
46. K. Villman, C. Blomqvist, R. Larsson and P. Nygren, *Anti-Cancer Drugs*, 2005, **16**, 609-615.

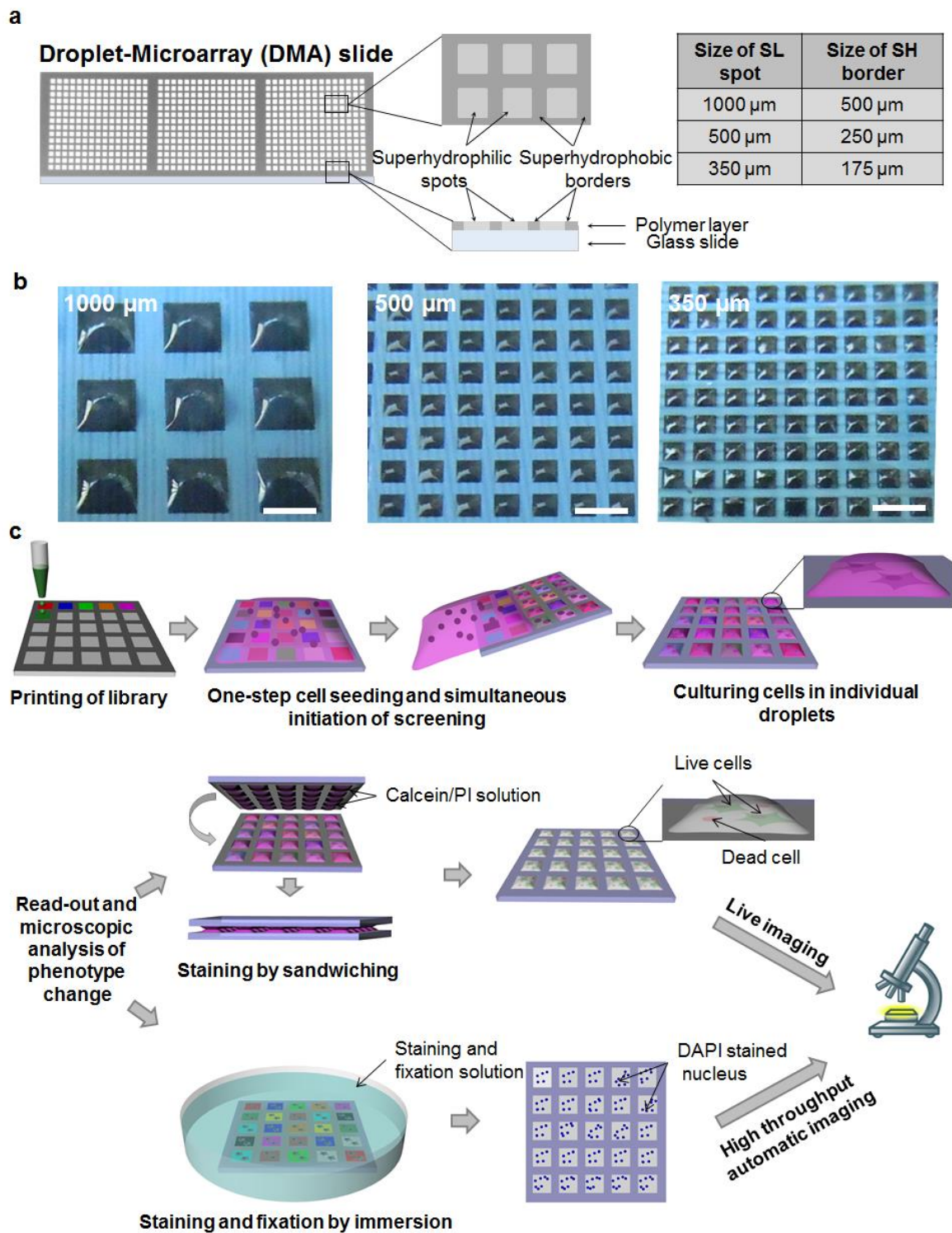


Fig. 1 Droplet-Microarray (DMA) reverse cell screening platform. (a) Schematic representation of a DMA slide and a table showing sizes of superhydrophilic spots and corresponding superhydrophobic borders. (b) Photographs of droplet microarrays. Scale bar 1 mm. (c) Schematic diagram of the workflow of reverse cell screening using DMA platform.

Fig. 2. Homogeneity of droplet formation and cell seeding on DMA. (a) Heights and volumes of water droplets on DMA with different spot sizes. (b) Lateral images of water droplets on DMA with different spot sizes. Scale bar, 1 mm. (c-d) Color-coded maps showing spatial distribution of cells between droplets and graphs showing distribution of cells on Droplet-Microarray containing 14x14 spots of 1000 μm size (c), 27x27 spots of 500 μm size (d) and 39x39 spots of 350 μm size (e). Numbers in squares represent number of cells per droplet. Bold square on color-coded map define area of the slide suitable for analysis.

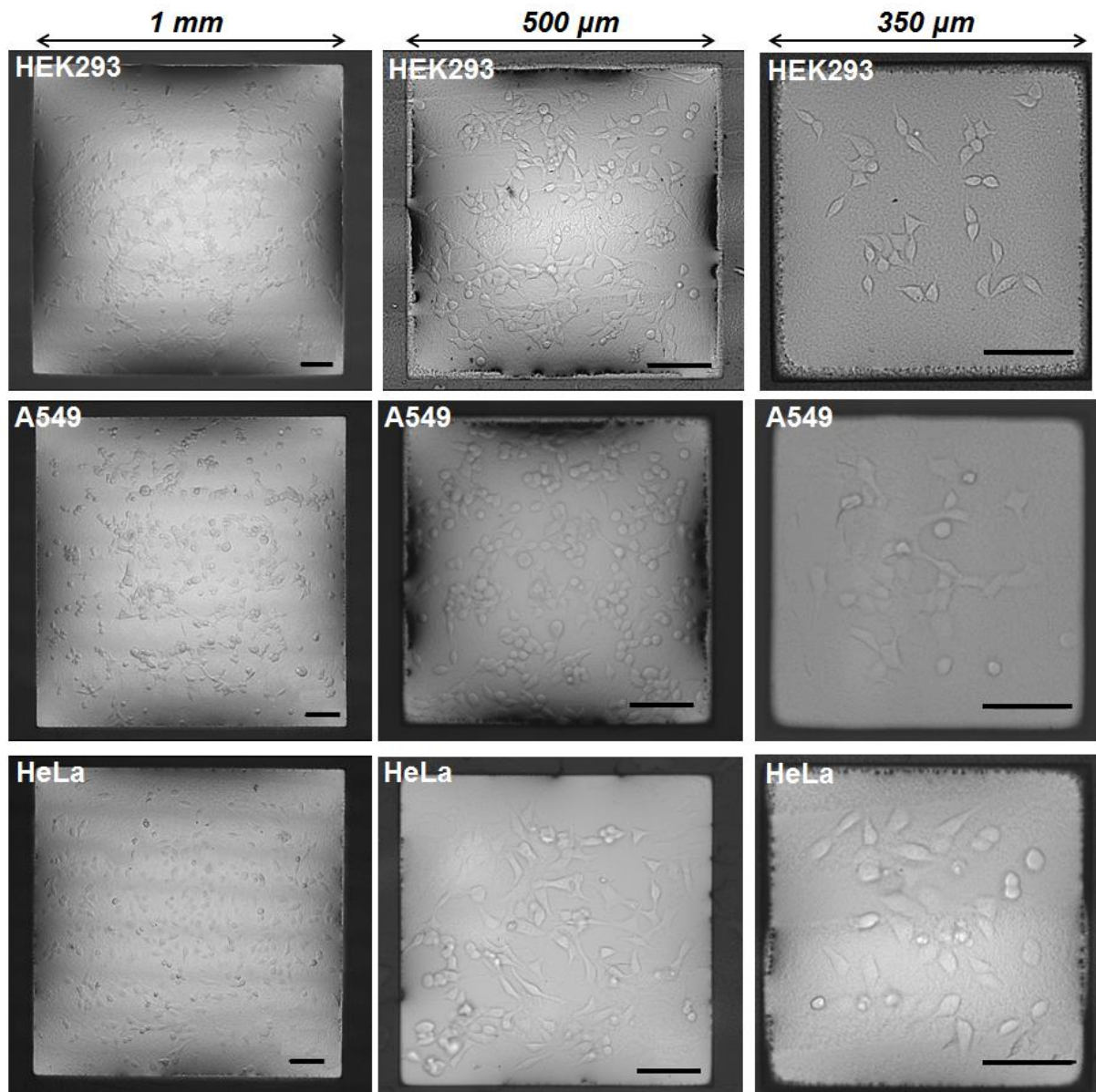


Fig. 3 Microscope images of HEK293, A549 and HeLa cells cultured in droplets of different sizes for 24 hours. Scale bar 100 μm .

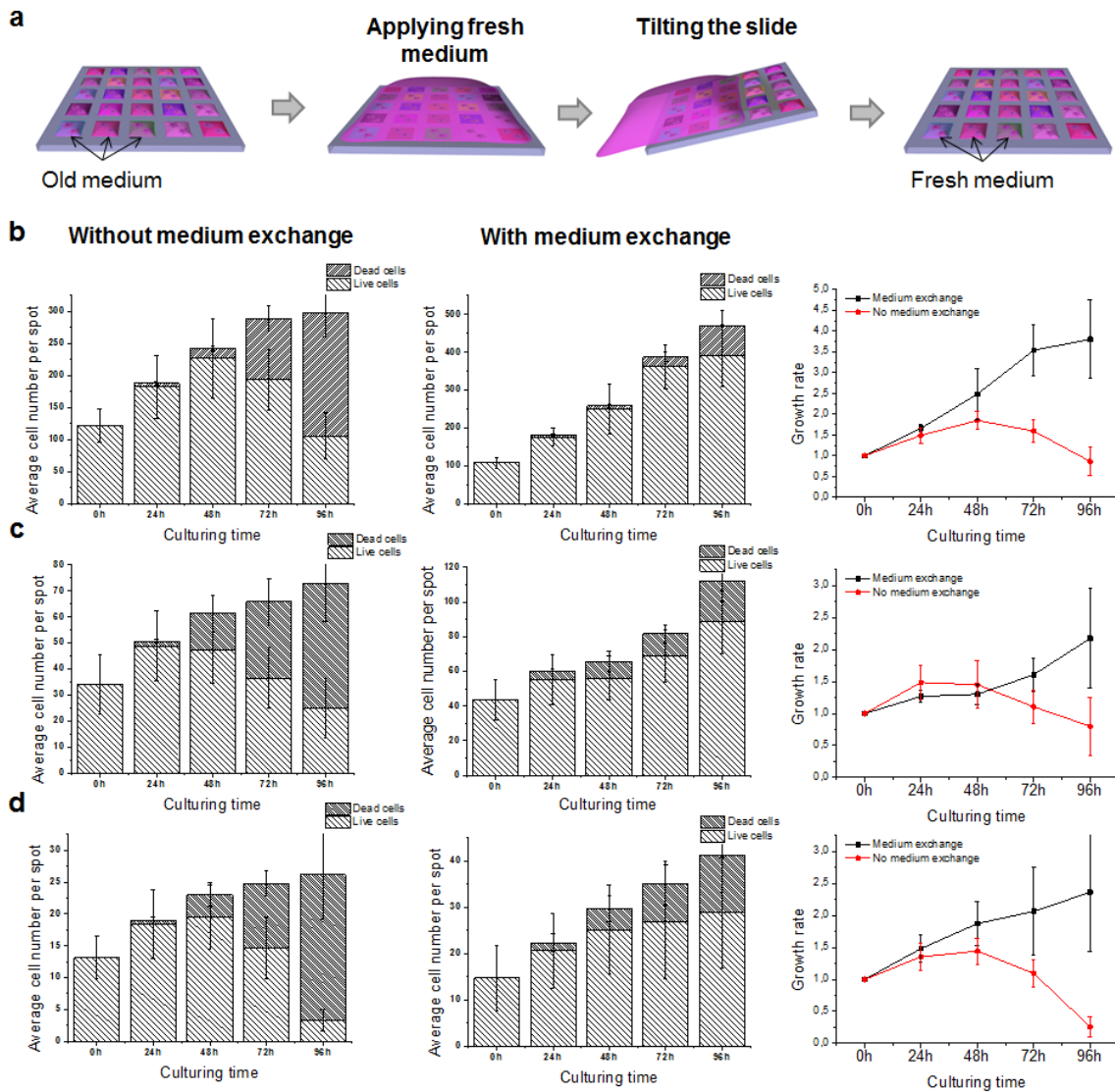


Fig. 4 Growth rate and viability of HeLa cells cultured using Droplet-Microarrays with different spot sizes. (a) Schematic diagram of medium exchange on Droplet-Microarray. (b-d) Growth rate and viability of HeLa cells cultured on Droplet-Microarray with spot sizes 1000 μm (b), 500 μm (c) and 350 μm (d). Graphs are showing growth rate of cells without (left) and with (middle) medium exchange and comparison of cell growth rates with and without medium exchange (right).

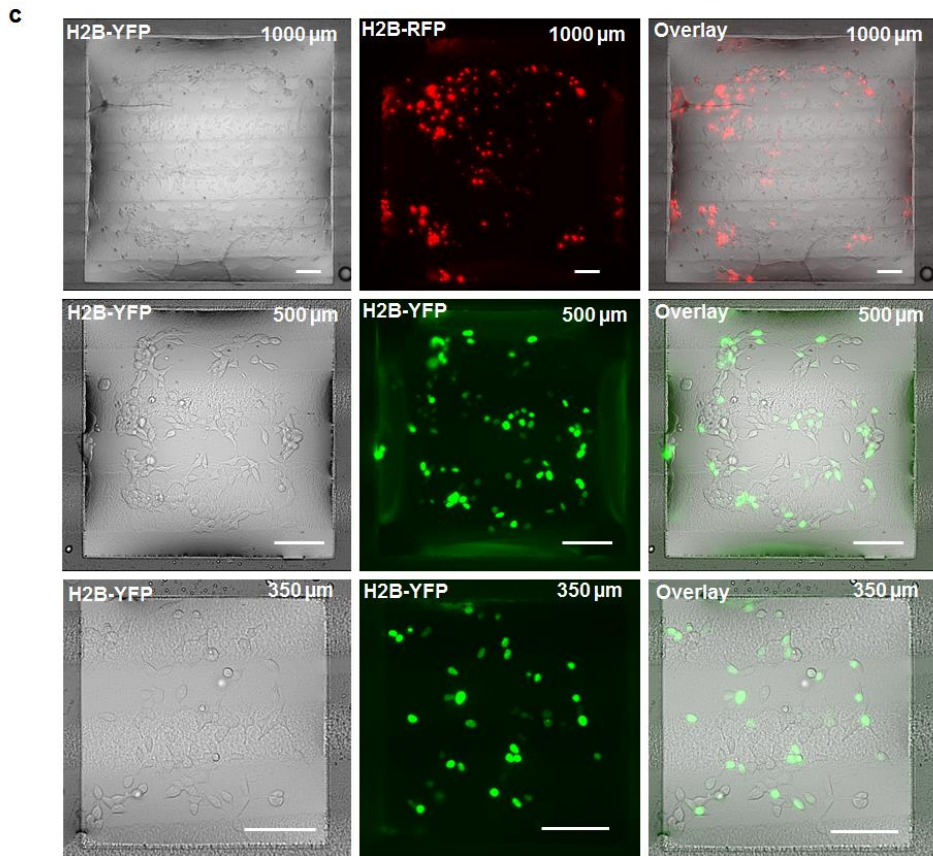
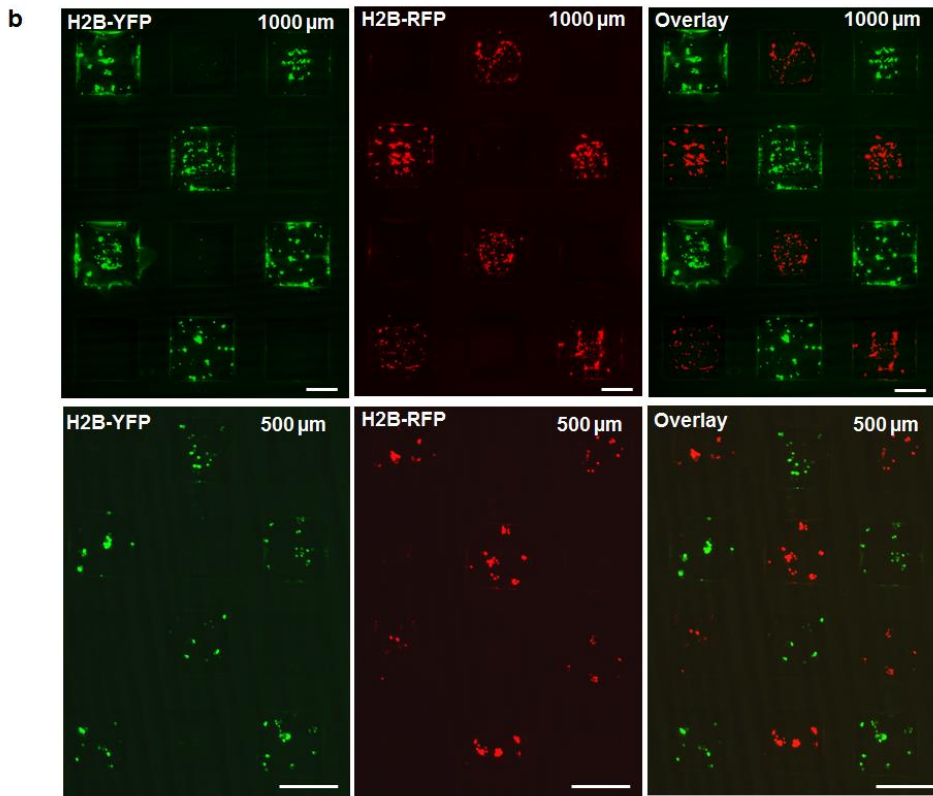
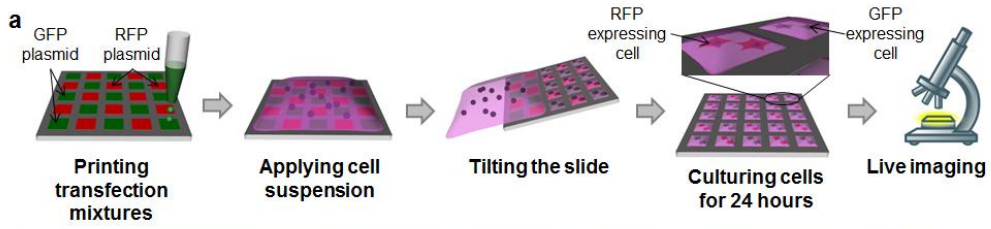


Fig. 5 Reverse cell transfection using Droplet-Microarray. (a) Schematic diagram of experimental workflow. (b) Fluorescence microscope images of HEK293 cells transfected with pCS2-H2B-YFP (green) or pCS2-H2B-RFP (red) on Droplet-Microarray with 1000 μm (top) and 500 μm (bottom) spot size in a checkerboard pattern. (c) Microscope images of individual droplets containing HEK293 cells transfected with pCS2-H2B-YFP (green) or pCS2-H2B-RFP (red) on DMA slides with different spot sizes (1000 μm , 500 μm and 350 μm).

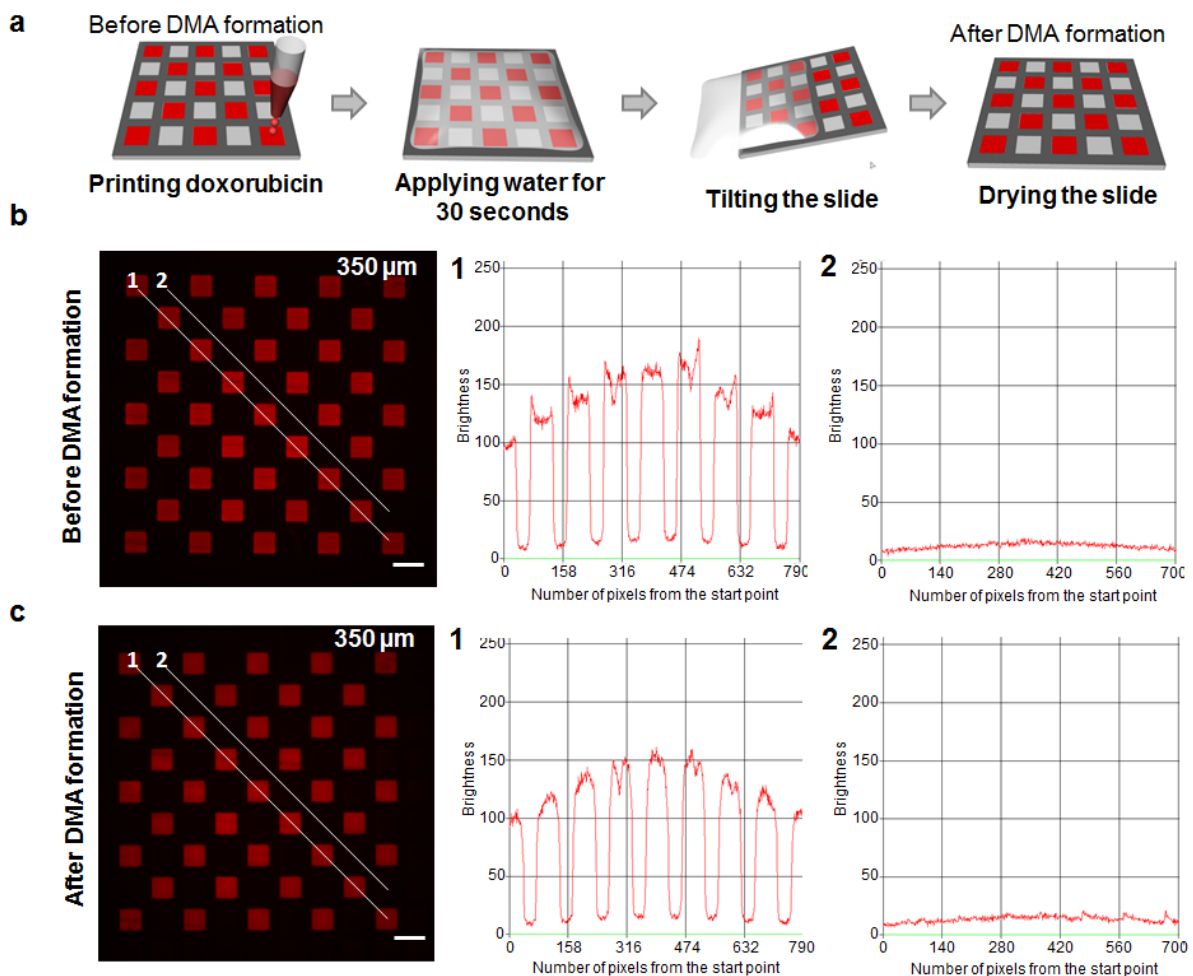


Figure 6. Cross-contamination study. (a) Schematic diagram of experimental workflow. (b, c) Microscopic image of DMA slide with spot sizes of 350 μm containing pre-printed doxorubicin in water solution (red) and fluorescence line profile of lines 1 and 2 indicated on the corresponding microscope image before DMA formation (b) and after DMA formation (c) Scale bar 500 μm .

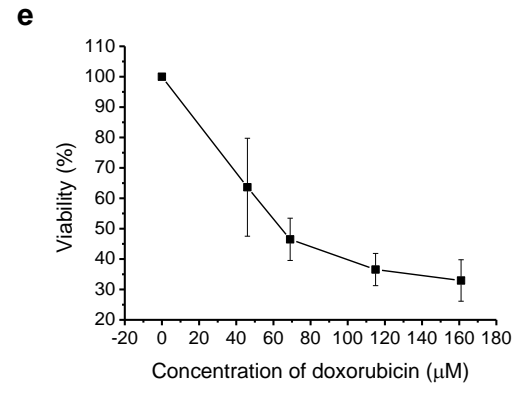
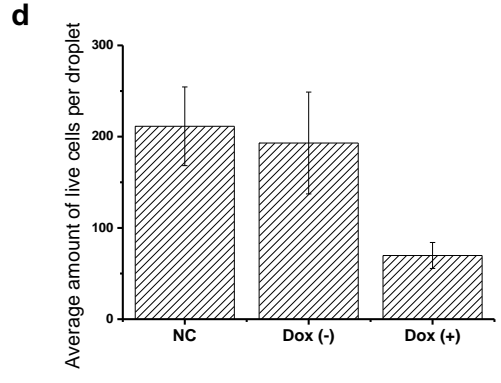
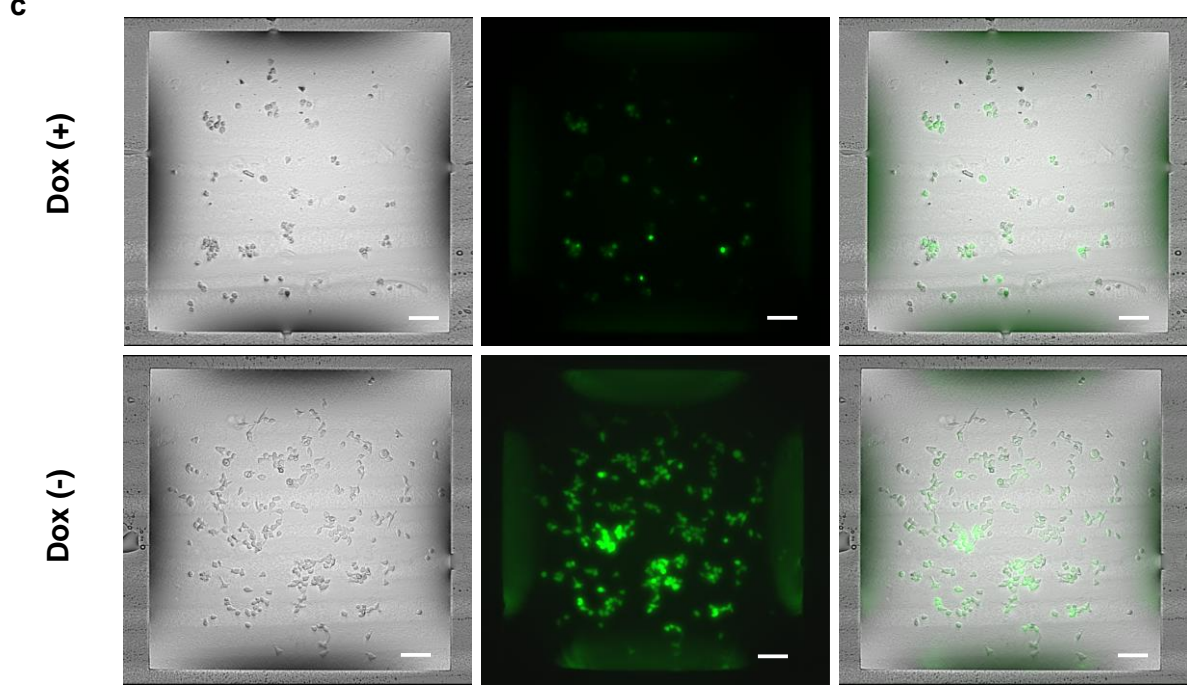
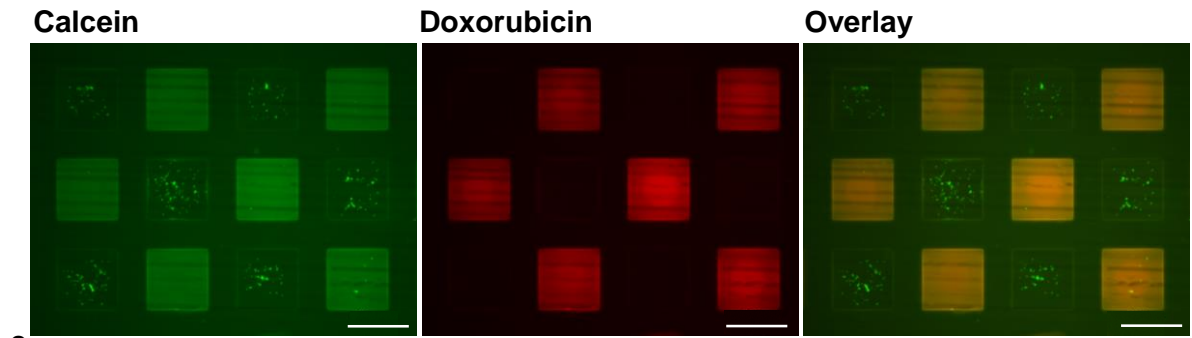
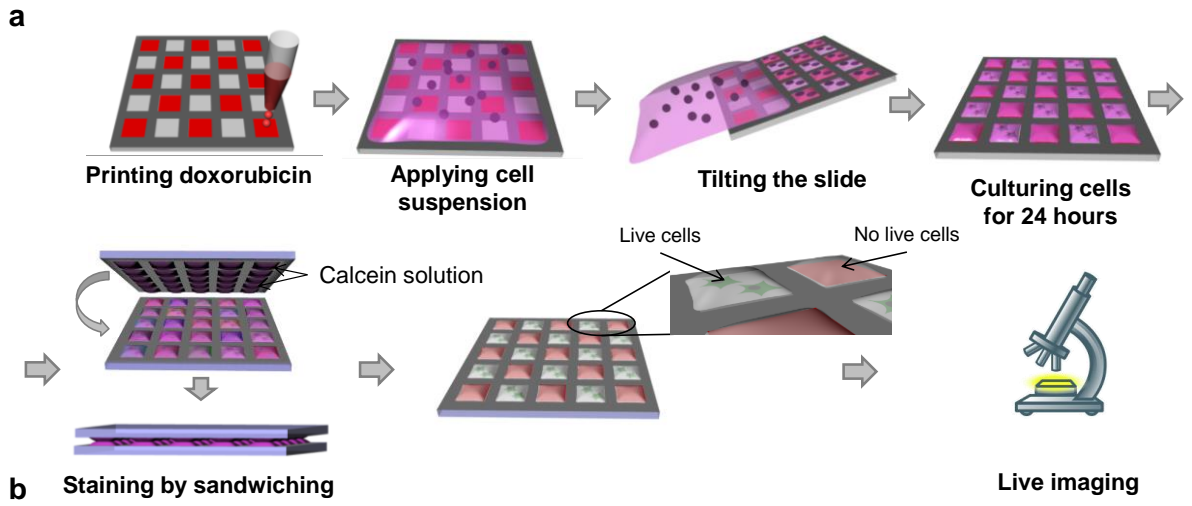


Figure 7. Treatment of cells with doxorubicin on Droplet-Microarray. (a) Schematic diagram of experimental workflow. (b) Microscopic images of calcein staining of HeLa cells 24 hours after seeding on Droplet-Microarray with preprinted doxorubicin (shows in red) in checkerboard pattern. (c) Microscopic images of calcein staining of individual doxorubicin positive and negative droplets containing HeLa cells 24 hours after seeding. (d) Comparison of the number of live cells in droplets on a negative control (NC) slide (one that contained no preprinted doxorubicin), in doxorubicin-negative droplets and doxorubicin-positive droplets. (e) Concentration-dependent effect of doxorubicin on viability of HeLa cells.